ISSN 2963-7511
Journal of Engineering Researcher and Lecturer, Vol. 2, No. 1, pp. 35-42, 2023

Investigation the maximum load capacity of the tail-shaft on the apron feeder using Solidwork simulations

Nailul Hidayat[1*], Primawati[1] and Phyo Wai Myint[2]

[1] Department of Mechanical Engineering, Faculty of Engineering, Universitas Negeri Padang, **INDONESIA**
[2] Department of Mechanical Engineering, Yangon Technological University, **MYANMAR**

Abstract: The tail-shaft is one of the components of the apron feeder on the conveyor. Its role is quite significant, as it includes a take-up system to adjust the tension and slackness of the chain on the sprocket against the Lamella. Based on observations in a mining industry, it was found that tail-shaft damage frequently occurs, likely due to the excess load carried by the conveyor. Therefore, researchers were interested in investigating the maximum capacity of the tail-shaft. The research was conducted using the Finite Element Analysis method with Solidworks Research License. The material used for the tail-shaft is DIN 1.0038. Torque variations tested on the tail-shaft were from 42,000 N.m to 58,000 N.m. Based on the simulation results, the maximum torque that the tail-shaft can withstand is 54,000 N.m with a safety factor value greater than 1, whereas when given a torque of 58,000 N.m, the safety factor value is less than 1. The tail-shaft experiences a maximum stress that exceeds the yield strength of DIN 1.0038 material, which can cause damage to the material. The initial damage appears at the end of the shaft due to the use of chamfer. This is known based on the results of simulations that have been conducted.

Keywords*:* Tail-shaft; FEA; Solidworks; Conveyor

*Corresponding Author: nailulhidayat2017@gmail.com

Received 20th February 2023; Revised: 04th April 2023; Accepted: 26th April 2023
https://doi.org/10.58712/jerel.v2i1.13

Reference to this paper should be made as follows: Hidayat, N., Primawati, & Myint, P. W. Investigation the maximum load capacity of the tail-shaft on the apron feeder using Solidwork simulations. *Journal of Engineering Researcher and Lecturer*, 2(1), 35–42. https://doi.org/10.58712/jerel.v2i1.13

1. Introduction

Conveyor is a transportation tool used to carry objects or materials from one place to another. Conveyors are widely used in various industries, including the mining industry. Conveyors are essential equipment in mining operations because they can efficiently and quickly transport materials from one location to another. Therefore, the use of conveyors in the mining industry is becoming more widespread and has become a commonly used tool (Mu et al., 2020). Conveyors have high transport efficiency and strong transport capacity (He et al., 2017). The function of this conveyor is essential for the mining industry as it can continuously transport materials. Therefore, a comprehensive study of the effectiveness and workability of the conveyor is required (Hrabovský et al., 2023).

In conveyor operations, it is not easy to measure the evenness of the transported material (Hrabovsky et al., 2022). In complex mining environments, conveyors often experience damage, such as overloading (He et al., 2017). Damage to the conveyor can halt the entire mining process (Wang & Zhang, 2012; Yang et al., 2020). Based on observations at a mining company, one component of the conveyor that frequently experiences damage is the tail-shaft. According to interviews with conveyor operators, the damage is caused by frequent overloading due to difficulty controlling the transported material. In a conveyor system, the tail shaft is used as a connector for the sprocket, which functions as a rotator and regulates the tension of the belt. The ideal belt tension will affect the durability of the conveyor's movement (Munzenberger et al., 2019) and its lifespan (Galkin & Sheshko, 2016).

Based on the factual issues that occur in the mining industry, this research aims to examine the maximum load that can be transported by the conveyor based on the maximum torque that can be sustained by the tail-Shaft. This work will be beneficial for optimizing conveyor design and providing information for mining operators in determining the limit of the material mass that can be transported.

2. Methods

This research was conducted using finite element analysis method using Solidworks Research License 2021-2022. The study was carried out by identifying the maximum torque that can be sustained by the tail-shaft based on the load of material transported by the conveyor.

2.1 Tail-shaft

The tail-shaft is one of the components of the take-up station, where its shape is depicted in Figure 1. This Take-up station consists of a Side Block, Sprocket, and tail-shaft.

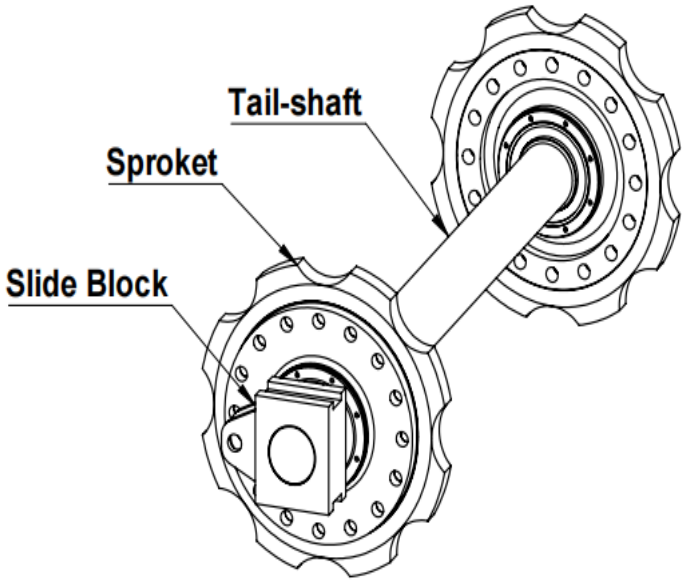

Figure 1. Take-Up station on apron feeder

The dimensions of the tail-shaft used in a mining company are shown in Figure 2. The tail-shaft has a length of 2689 mm, with a diameter of 180 mm in the middle section along 1897 mm, and both ends have a diameter of 160 mm along 397 mm.

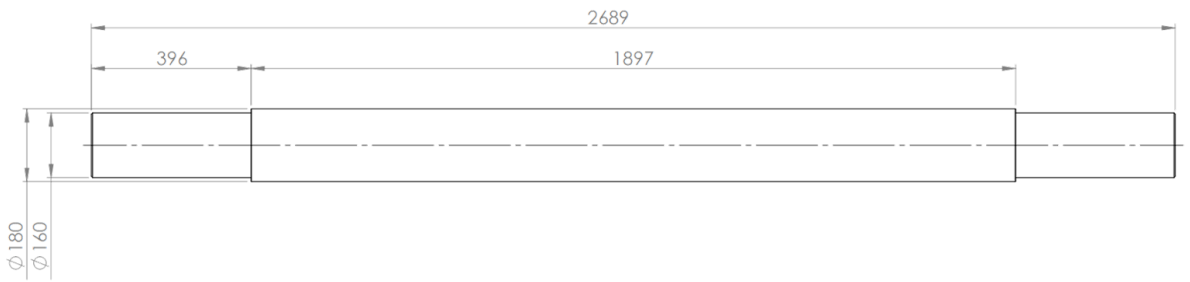

Figure 2.Tail-shaft

The material used for the tail-shaft is DIN 1.0038. The material properties are presented in Table 1.

Table 1. Material properties of DIN 1.0038

Property	Value
Elastic modulus	210000 N/mm^2
Poisson' ratio	0.28
Shear modulus	79000 N/mm^2
Mass density	7800 Kg/M^3
Tensile strength	360 N/mm^2
Yield strength	235 N/mm^2

2.2 Torque on tail-shaft based on material load

The torque acting on the shaft is calculated based on the mass of material transported by the conveyor. The equation used to determine the torque value on the tail-shaft is as follows:

$$\tau = F \times L \quad (1)$$

The torque (T) is the product of the force (F) and the length (L) of the tail-shaft. To calculate the force, the following equation is used:

$$F = m \times g \quad (2)$$

The force (F) acting on the tail-shaft is the mass of the transported material (m) multiplied by gravity (g). The variation of torque experienced by the tail-shaft based on the mass carried by the conveyor is presented in Table 2.

Tabel 2. Torque on a tail-shaft based on load

Mass (Kg)	Force (N)	Torsi (Nm)
1.597,51	15.671,64	42.000
1.749,66	17.164,17	46.000
1.901,80	18.656,71	50.000
2.053,95	20.149,25	54.000
2.206,09	21.641,79	58.000

2.3 Mesh independent test

The mesh element size used is selected based on a mesh independent test. This is done to obtain more accurate simulation results while still maintaining efficient computation time.

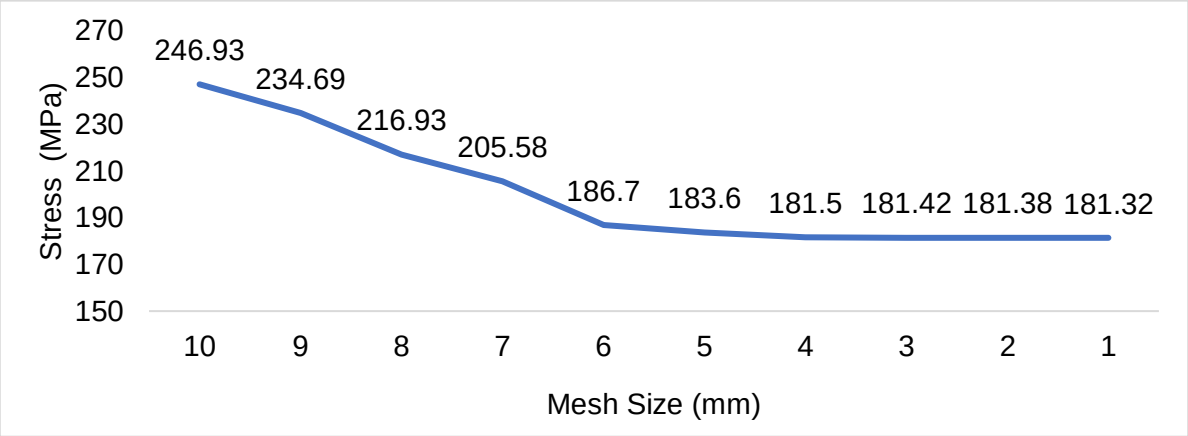

Figure 3. Mesh independent test

The mesh independent test is performed by using several different mesh element sizes, ranging from coarse to very fine. The mesh parameter used is Standard mesh, as the shape of the tail-shaft is simple and does not have extreme curves. The comparison between mesh size (mm) and stress (MPa) that occurs during the simulation with a torque moment of 42,000 Nm is presented in Figure 3. Based on the simulation results at the same torque moment with different mesh sizes, a mesh size of 4 mm is determined. This is because at this mesh size, the maximum stress that occurs is not significantly different from the smaller mesh size (1 mm). The selection of the appropriate mesh size is important in ensuring accurate simulation results without sacrificing computational efficiency.

3. Results and discussion

3.1 Stress

The tail-shaft, which experienced a torque of 42,000 N.m, exhibited a maximum stress of 181.50 MPa, as shown in Figure 4(a) simulation. Figure 4(b) shows the simulation result for a torque of 46,000 N.m, with a maximum stress of 198.78 MPa experienced by the tail-shaft. For the Tail-Shaft with a torque of 50,000 N.m, the maximum stress experienced was 216.07 MPa (Figure 4(c)). A torque of 54,000 N.m resulted in a maximum stress of 233.36 MPa for the Tail-Shaft (Figure 4(d)), while a torque of 58,000 N.m resulted in a stress of 250.64 MPa experienced by the tail-shaft (Figure 4(e)). The simulation results, which varied the torque experienced by the tail-shaft, indicate that as the torque increases, so does the stress experience by the tail-shaft.

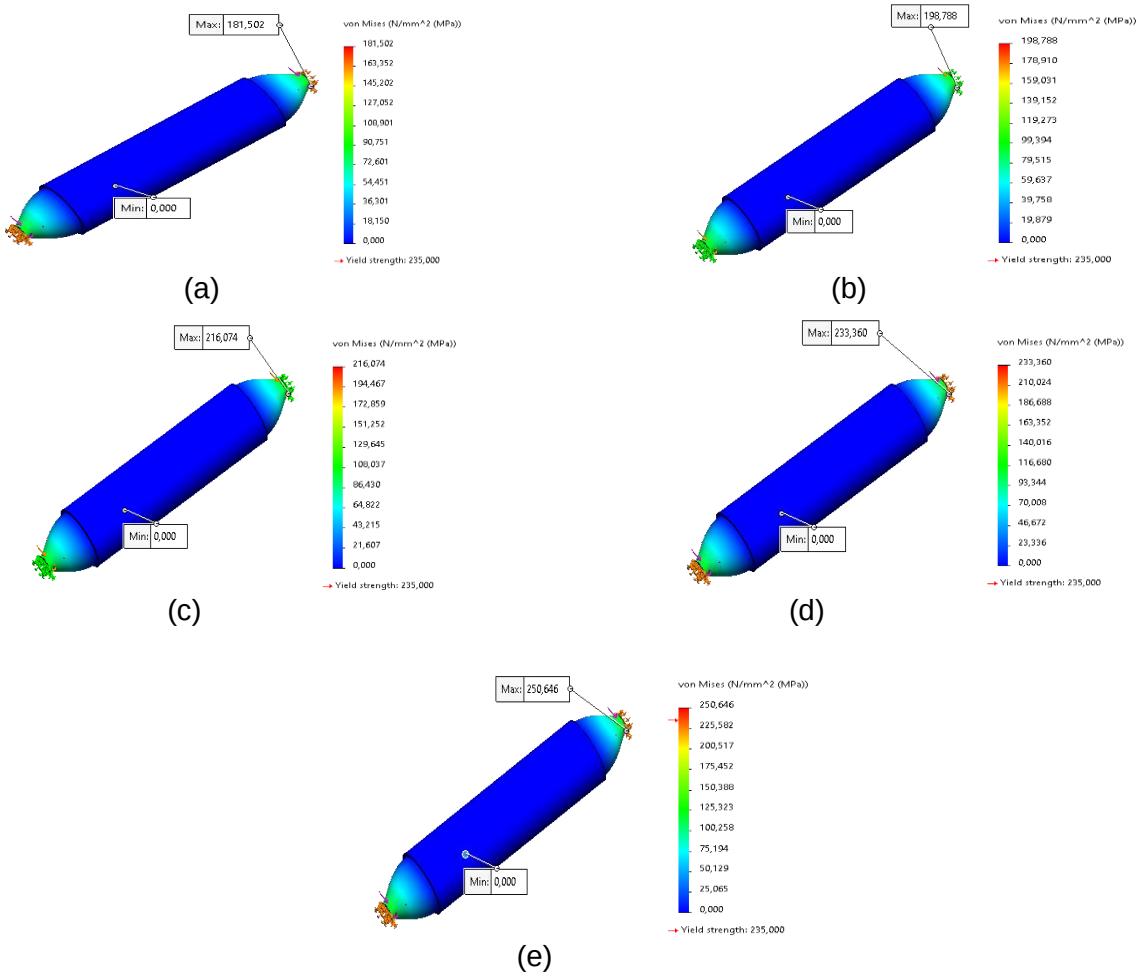

Figure 4. Stress tail-shaft

3.2 Displacement

The maximum displacement experienced by the tail-shaft after receiving a torque of 42,000 N.m is 0.142 mm (Figure 5(a)). At a torque of 46,000 N.m, the tail-shaft experienced a maximum displacement of 0.155 mm (Figure 5(b)), while at a torque of 50,000 N.m, the displacement that occurred on the tail-shaft was 0.169 mm (Figure 5(c)). Furthermore, at a torque of 54,000 N.m, the displacement experienced by the tail-shaft was 0.182 mm, and at a torque of 58,000 N.m, the displacement that occurred was 0.196 mm. Similar to stress, as the torque experienced by the tail-shaft increases, the displacement also increases.

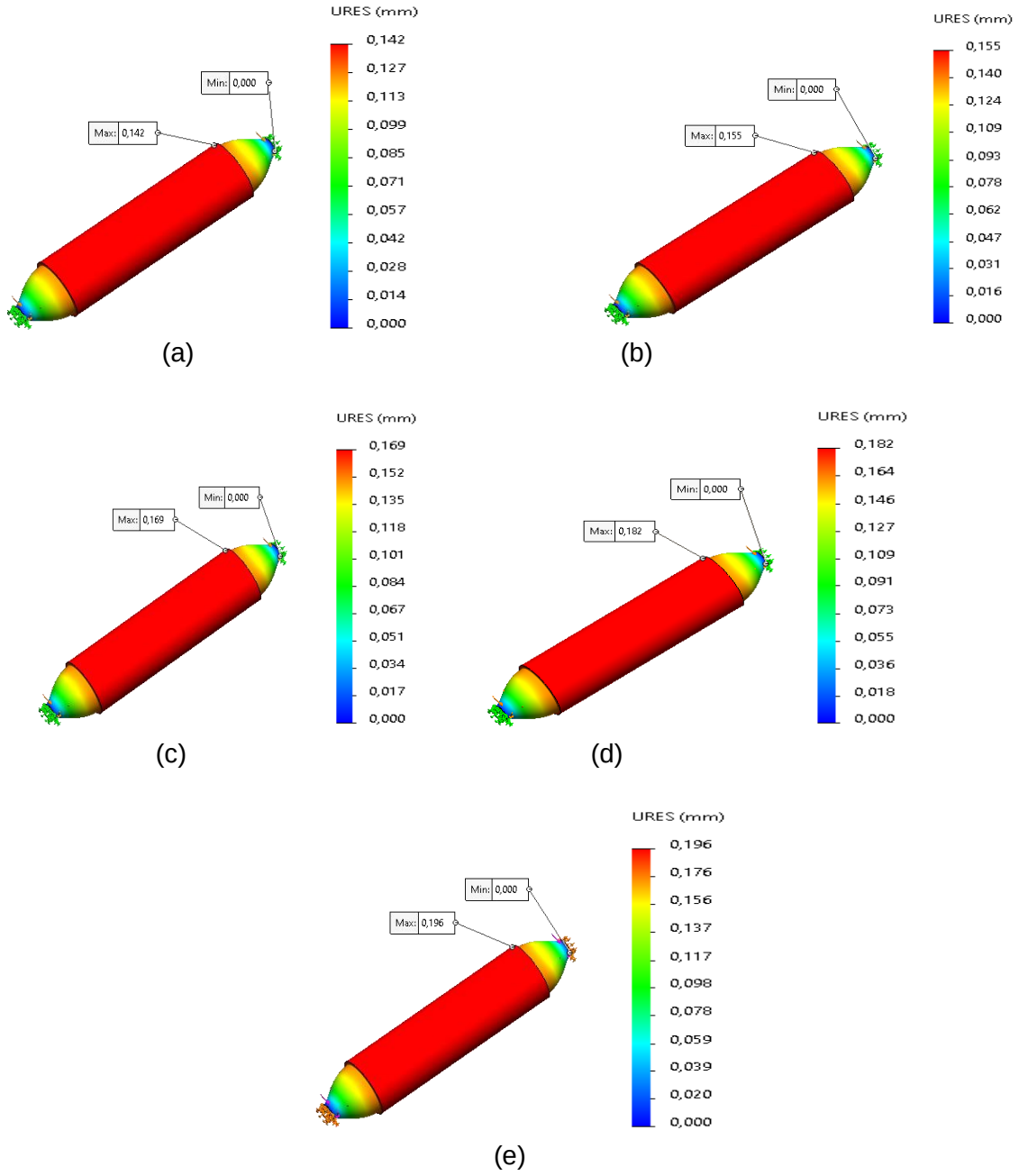

Figure 5. Displacement tail-shaft

3.3 Safety factor

The safety factor is a value that represents the ability of a configuration to withstand loads.

Based on the simulation results, out of the five torque variations applied to the tail-shaft, only at a torque of 58,000 N.m did the safety factor value fall below 1, specifically to 0.938. When the tail-shaft received a torque of 54,000 N.m, the obtained safety factor value was 1.007, while for a torque of 50,000 N.m, the safety factor value was 1.088. For a torque of 46,000 N.m, the safety factor value was 1.182, and for a torque of 42,000 N.m, the safety factor value was 1.295.

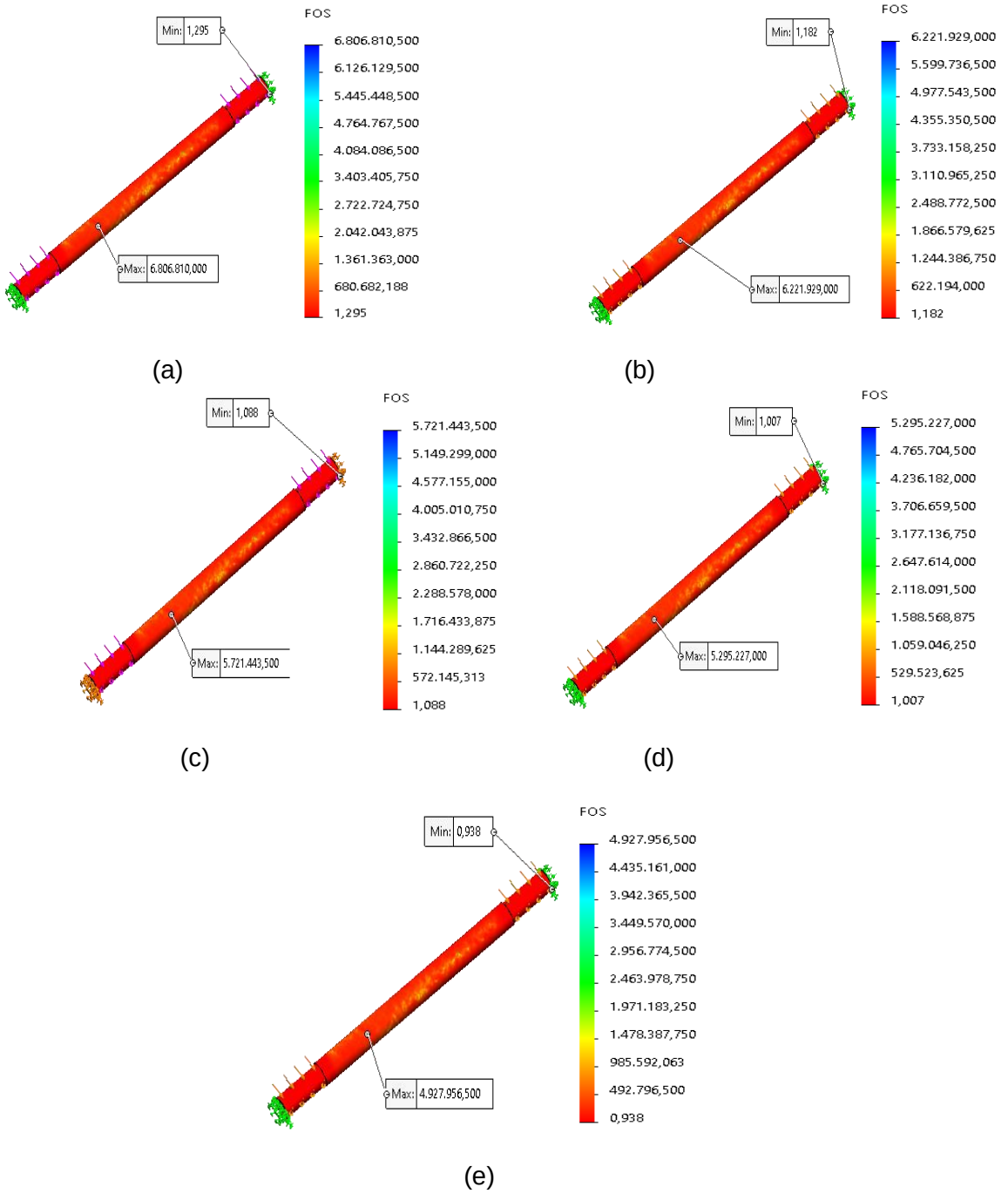

Figure 6. Safety factor

The tail-shaft with a torque of 58,000 N.m, which has a safety factor less than 1, experiences initial cracking at the end due to the use of chamfer (refer to Figure 7). The research findings indicate that the initial cracking due to the torsional load on the stepped shaft occurred at the chamfer (Saiful et al., 2021). The crack will propagate to other parts of the shaft, which can

result in failure or breakage of the shaft. Stress concentration can be reduced by rounding the outer angle appropriately (fillet) (Huth, 1950).

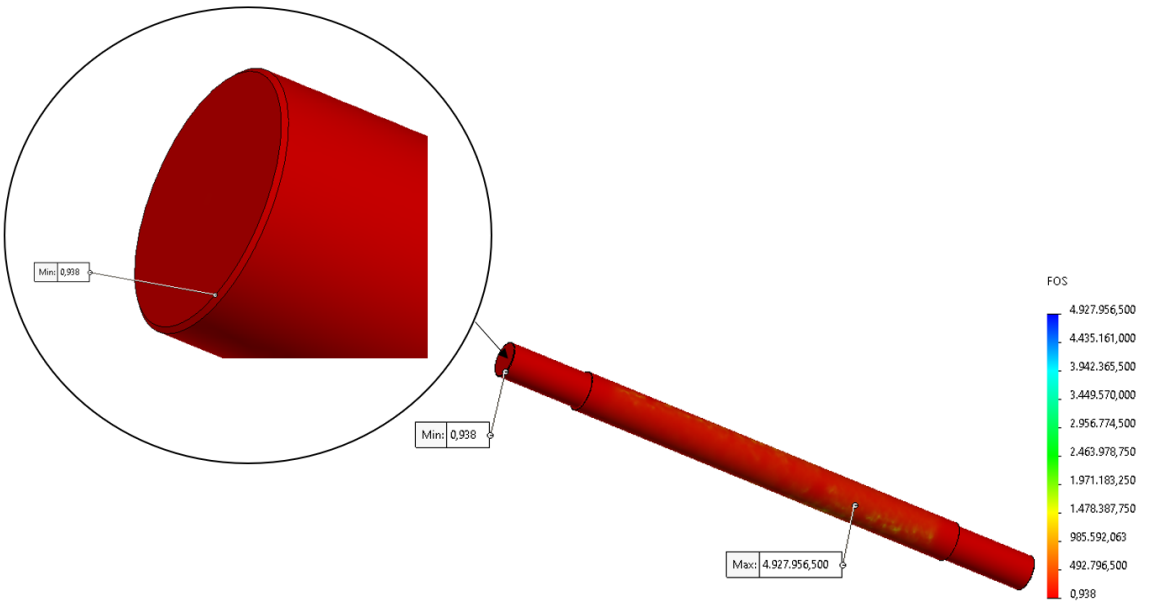

Figure 7. The part of the tail-shaft that has a safety factor > 1

The tail-shaft is a multilevel shaft. When a multilevel shaft is subjected to continuous torsional fatigue with a torque that exceeds the material's strength limit, it can cause cracking on the shaft's surface, which can ultimately lead to total failure. DIN 1.0038, the material used for the tail-shaft, is a low-carbon steel with relatively low tensile strength. At a torque of 58,000 N.m, the stress experienced by the tail-shaft exceeds the material's elastic limit, resulting in permanent deformation that will not return to its original shape. If the torsional load applied to the multilevel shaft is not uniform, it can cause distortion on the shaft, which can eventually lead to cracking. When the torsional load applied to the multilevel shaft exceeds the material's strength limit, the shaft can break or crack suddenly. This can occur because the mass of material carried by the conveyor in each bucket is not the same.

4. Conclusions

The testing of the maximum torque that the tail-shaft can withstand is crucial as exceeding its capacity can result in breakage and disrupt mining or production processes. Based on the simulation results, the tail-shaft can withstand a maximum torque of 54,000 N.m, with the maximum stress occurring at 233.36 MPa and the safety factor value being greater than 1. According to the FAE simulation conducted, the conveyor's maximum capacity to transport material is 2,053.95 kg. The failure of the tail-shaft is caused by the failure at the end of the shaft due to the use of Chamfer. Damage can be prevented by creating a fillet shape at the end of the shaft in a carefully crafted manner.

Acknowledgements

The author would like to express the utmost gratitude to the Manufacturing Laboratory of Universitas Negeri Padang for providing the facilities to conduct computer simulation and Solidworks Research License. Special thanks are also extended to the design and manufacture research team for providing valuable advice and inputs for the writing of this research article.

Declarations

Author contribution

Nailul Hidayat acted as the author of the article, designer of the Tail-Shaft, and performer of the simulation. Primawati contributed to data processing and interpretation of simulation results. Phyo Wai Myint provided inputs on the mesh independent test, discussion of simulation data, and article evaluation.

Funding statement

This research received no specific grant from any funding agency in the public, commercial, or not-for-profit sectors.

Complict of interest

The author declares no conflict of interest.

Ethical clerance

There are no human subjects in this manuscript and informed consent is not applicable.

References

Galkin, V. I., & Sheshko, E. E. (2016). Substantiation of key design and regime parameters of sandwich belt high-angle conveyors. *Gornyi Zhurnal*, 73–77. https://doi.org/10.17580/gzh.2016.12.15

He, D., Pang, Y., & Lodewijks, G. (2017). Green operations of belt conveyors by means of speed control. *Applied Energy*, *188*, 330–341. https://doi.org/10.1016/j.apenergy.2016.12.017

Hrabovský, L., Blata, J., Hrabec, L., & Fries, J. (2023). The detection of forces acting on conveyor rollers of a laboratory device simulating the vertical section of a Sandwich Belt Conveyor. *Measurement*, *207*, 112376. https://doi.org/10.1016/j.measurement.2022.112376

Hrabovsky, L., Molnar, V., Fedorko, G., Tkac, J., & Frydrysek, K. (2022). Experimental determination of force acting on a sandwich conveyor's pressure roller in transport of bulk materials for the needs of failure analysis. *Measurement*, *202*, 111832. https://doi.org/10.1016/j.measurement.2022.111832

Huth, J. H. (1950). Torsional Stress Concentration in Angle and Square Tube Fillets. *Journal of Applied Mechanics*, *17*(4), 388–390. https://doi.org/10.1115/1.4010164

Mu, Y., Yao, T., Jia, H., Yu, X., Zhao, B., Zhang, X., Ni, C., & Du, L. (2020). Optimal scheduling method for belt conveyor system in coal mine considering silo virtual energy storage. *Applied Energy*, *275*, 115368. https://doi.org/10.1016/j.apenergy.2020.115368

Munzenberger, P. J., O'Shea, J. I., & Wheeler, C. A. (2019). A comparison of rubber stress relaxation models for conveyor belt indentation rolling resistance calculations. *International Journal of Mechanics and Materials in Design*, *15*(2), 213–224. https://doi.org/10.1007/S10999-018-9412-Y/METRICS

Saiful, W., Husaini, & Nurdin, A. (2021). Failure analysis on the fracture shaft of a centrifugal pump used for diesel engine cooling system. *Key Engineering Materials*, *892 KEM*. https://doi.org/10.4028/www.scientific.net/KEM.892.107

Wang, C. Q., & Zhang, J. (2012). The Research on the Monitoring System for Conveyor Belt Based on Pattern Recognition. *Advanced Materials Research*, *466–467*, 622–625. https://doi.org/10.4028/www.scientific.net/AMR.466-467.622

Yang, R., Qiao, T., Pang, Y., Yang, Y., Zhang, H., & Yan, G. (2020). Infrared spectrum analysis method for detection and early warning of longitudinal tear of mine conveyor belt. *Measurement*, *165*, 107856. https://doi.org/10.1016/j.measurement.2020.107856